

pubs.acs.org/Macromolecules Article

# Polyhalohydrins: Investigating Vicinal Functionalities by Ring-Opening of Epoxides on Polyolefins

Anne N. Radzanowski,<sup>#</sup> Hoda Shokrollahzadeh Behbahani,<sup>#</sup> William McCambridge, Clay Gensel, Catherine Spence, Karen I. Winey,\* and E. Bryan Coughlin\*



Cite This: Macromolecules 2025, 58, 10073-10083



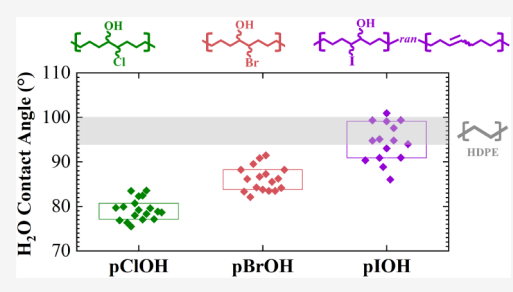
**ACCESS** I

III Metrics & More

Article Recommendations

s Supporting Information

ABSTRACT: Halohydrins are functional groups that are underexplored in polymer science. This study synthesized and examined structure—property relationships of halohydrin-functionalized polymers derived from polycyclooctene (PCOE), which was obtained via ring-opening metathesis polymerization (ROMP). The polyhalohydrins, including polychlorohydrin, polybromohydrin, and polyiodohydrin, were produced through a two-step process involving epoxidation of PCOE followed by epoxide ring-opening using hydrochloric, hydrobromic, or hydroiodic acid. These stereoirregular and regioirregular polymers are amorphous as measured by differential scanning calorimetry and X-ray scattering. Lap joint shear testing revealed an enhanced adhesive



performance in polychlorohydrin and polybromohydrin, with the former demonstrating nearly three times the ultimate shear stress compared to a model polyethylene, hydrogenated PCOE. Additionally, contact angle measurements and surface free energy analysis showed an increase in hydrophilicity and polarity from iodine- to bromine- to chlorine-functionalized polyhalohydrins, aligning with trends in adhesion strength. These results underscore the potential of halohydrin functionalization as a versatile approach for tuning surface properties, offering new opportunities for polymer-to-polymer transformations.

## ■ INTRODUCTION

The identity and placement of functional groups along a polymer backbone are known to impact polymer properties and performance. Polymerization of vinyl monomers results in regioregular polymers with a substituent(s) placed on every other carbon along the polymer backbone. Another microstructural characteristic of vinyl polymers is stereoirregularity (atactic) and stereoregularity (isotactic or syndiotactic). Finally, 1,1-disubstituted vinyl monomers (i.e., methyl methacrylate) result in polymers with geminally substituted carbons placed at every other backbone carbon.

Notably, copolymerization of vinyl monomers with ethylene results in the placement of substituents further apart than on every other backbone carbon. Poly(ethylene-co-vinyl alcohol) (EVOH) is a widely used commercial polymer known for its oxygen barrier properties and utility in multilayer packaging, Figure 1.2,3 Commercial EVOH is a branched polymer produced by the copolymerization of ethylene and vinyl acetate followed by hydrolysis to the vinyl alcohol, typically with vinyl alcohol levels from 52 to 72 mol %.4,5 A specific subset of EVOH, polymers with vicinal hydroxyl functionality, equivalent to 50 mol % vinyl alcohol, was recently published by our groups and found that the thermal properties and crystallinity of these polymers were highly dependent on the stereochemistry of the diols within the backbone.<sup>6</sup> Rather than copolymerization, chlorinated polyethylene (CPE) is synthesized from the chlorination of a high-density polyethylene using a free-radical aqueous slurry technique, Figure 1.<sup>7</sup> At low levels of chlorination (16–24 mol %) the polymer behaves as a thermoplastic elastomer.<sup>7</sup> When the level of chlorination is increased, the polymer becomes more elastomeric, while at very high chlorine content (>70 mol %), the polymer is brittle.<sup>7</sup> The chlorine content is tailored depending on the desired properties and applications.

Though EVOH and CPE are produced in commercial quantities, much less is known about polymers with vicinal substituents of –OH or –Cl, wherein the functionality is on adjacent backbone carbons. Halohydrins are a molecular example of this kind of vicinal functionality, carrying a hydroxyl and a halide group on neighboring carbon atoms. Halohydrins are valuable functional groups in organic chemistry, specifically in the areas of pharmaceuticals, and their functionality has been known and understood for over 100 years. <sup>8,9</sup> Despite their importance to the field of molecular synthesis, halohydrins have not yet found broad utility as functional groups in polymer science.

Received: July 6, 2025
Revised: September 5, 2025
Accepted: September 8, 2025

Published: September 15, 2025





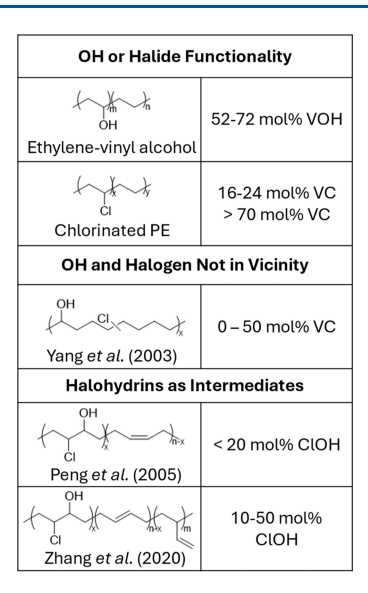


**Figure 1.** Commercial polymers that include either hydroxyl or halide functionality include poly(ethylene-*co*-vinyl alcohol) and chlorinated polyethylene. Other polymers include combinations of OH and halide functionality either not in the vicinity of each other or on adjacent carbon centers.

Small molecule halohydrins are synthesized through a variety of chemistries. One of the most common paths is via the ring-opening of epoxides with halo acids, such as hydrobromic or hydrochloric acid. 10,11 Epoxidation of double bonds within a polymer backbone is a well-understood and commonly performed transformation, providing ample opportunity for further elaboration. Recent halohydrin literature has investigated the use of biocatalysis using halohydrin dehalogenase enzymes to ring-open epoxides with a level of stereoselectivity and chemoselectivity necessary for pharmaceutical applications. Phenomena of enzymatic biocatalysis skips the halohydrin intermediate and can produce desired functionality through the inclusion of other nucleophiles. This chemistry is most prevalent in small molecule transformations.

Propylene chlorohydrin is an important intermediate for production of propylene oxide, polyether polyols, and eventually urethane polymerization. <sup>23,24</sup> As functional groups, however, polyhalohydrins are much less common, though not entirely unstudied. Previously, hydrochloric acid has been used to ring-open the epoxides of partially epoxidized polybutadiene for further elaboration, primarily by grafting reactions at the hydroxyl group. <sup>25,26</sup> Zhang et al. reacted monoisocyanates to the hydroxyl pendant groups of polybutadiene functionalized by epoxidation and hydrochloric acid ring-opening to generate noncovalent polymer networks with shape memory, Figure 1. <sup>26</sup> Their investigation focused on levels of modification between 10 and 50 mol %. <sup>26</sup>

Previously, Peng and Abetz also utilized a three-step pathway for the modification of polybutadiene to supramolecular hydrogen bonding networks, Figure 1.<sup>25</sup> Their degree of modification was lower than what was later reported by Zhang et al. with a maximum level of functionalization of 20 mol %.<sup>25,26</sup> The ring-opening of epoxides with hydrochloric acid has also been attempted on an epoxidized polynorbornene backbone, however those attempts were unsuccessful due to the bulkiness of the nearby norbornene.<sup>27</sup> There have been few efforts to thoroughly characterize the halohydrin intermediates,

and to our knowledge no examples of halohydrin functionalization of a polyethylene backbone without remaining double bonds have been investigated.

Earlier studies from Stephens et al. and Yang et al. investigated the synthesis and characterization of a chlorinated polyethylene backbone through the use of prefunctionalized cyclic olefin monomers. 28,29 Because they had used olefin metathesis polymerization the resulting polymers had both chlorine and alkene functionality, Figure 1. To access a polyethylene-like backbone with 0 to 50 mol % vinyl chloride, the double bonds were hydrogenated.<sup>29</sup> In general, as the mol % of vinyl chloride increased, the glass transition temperature increased, while the melting temperature and crystallinity decreased. Other experiments they performed involved hydroboration and oxidation of the double bonds to introduce hydroxyl groups, however this route does not produce the halohydrin functionality because the hydroxyl and halide were not on adjacent carbon centers.<sup>29</sup> These polymers were insufficiently soluble for thorough characterization beyond <sup>1</sup>H NMR spectroscopy.

This investigation describes the synthesis and characterization of three polyhalohydrins from fully epoxidized polycyclooctene, to both prepare these previously unexplored materials and examine the fundamental structure—property relationships associated with these novel functionalities. The epoxides were ring-opened by hydrochloric, hydrobromic, or hydroiodic acid. At complete functionalization, the polymers are analogous to linear poly(ethylene-co-vinyl alcohol-co-vinyl chloride), poly(ethylene-co-vinyl alcohol-co-vinyl bromide), or poly(ethylene-co-vinyl alcohol-co-vinyl iodide) terpolymers with (i) 50 mol % ethylene monomeric repeat units and (ii) only head-to-head coupling of the vinyl alcohol and vinyl halides. The polychlorohydrin, polybromohydrin, and polyiodohydrin will be referred to by the abbreviations pClOH, pBrOH, and pIOH, respectively.

# **EXPERIMENTAL METHODS**

**Materials.** Hydrochloric acid (HCl, 37%), hydrobromic acid (HBr, 48%), hydroiodic acid (HI, 57%), and L-ascorbic acid were purchased from Sigma-Aldrich and used as received. Tetrahydrofuran (THF) and sodium bicarbonate for polymer synthesis was obtained from Fisher Scientific and used as received. Deuterated chloroform (CDCl<sub>3</sub>) was purchased from Cambridge Isotope Laboratories. Polycyclooctene (PCOE) and epoxidized PCOE were prepared as described in the Supporting Information (Schemes S1 and S2). THF (≥99%, stabilized) was purchased from Alfa Aesar and used as received. Aluminum sheets for lap joints (1100 Aluminum, 1.6 mm thickness) were sourced from McMaster-Carr and cut into 120 mm × 25.4 mm coupons for lap joint shear testing. Tefzel (Ethylene tetrafluoroethylene, ETFE) films were purchased from CSHyde and used as received. Diiodomethane (CH<sub>2</sub>I<sub>2</sub>, ≥99%, stabilized) was purchased from Thermo Fisher Scientific and used as received.

Synthesis of Polychlorohydrin (pClOH). A 20 mL scintillation vial was charged with a stir bar and previously synthesized epoxidized PCOE (0.25 g, 0.0085 mmol). The polymer was dissolved in 10 mL of THF on a magnetic stir plate. Once dissolved, HCl (3.5 mL, 42 mmol) was added dropwise to the polymer solution. After 18 h, the solution was removed from the stir plate and precipitated dropwise in a 10-fold excess by volume of stirred deionized water. Sodium bicarbonate (3.5 g, 42 mmol) was added to the solution until a pH strip read as neutral. The solution was left to stir for 6 h to allow the polymer to collect on the stir bar and sides of the beaker. The polymer was collected by decanting off the water and dried overnight in the vacuum oven at 50 °C. The percent yield was 99%.  $M_{\rm n,NMR}$  = 7400 g/mol;  $^{\rm 1}$ H NMR (500 MHz, CDCl<sub>3</sub>)  $\delta$  4.08–3.95 (m, 1nH),

Scheme 1. Synthesis of Polychlorohydrin (pClOH), Polybromohydrin (pBrOH), and Polyiodohydrin (pIOH) by Ring-Opening of Epoxidized Polycyclooctene

3.95–3.87 (m, 1nH), 3.80–3.69 (m, 1nH), 3.68–3.57 (m, 1nH), 2.29–1.92 (br s, 1nH) 1.87–1.21 (m, 12nH), 1.12–1.06 (t, 6H), 1.06–0.97 (t, 6H) ppm;  $^{13}\mathrm{C}$  NMR (400 MHz, CDCl<sub>3</sub>)  $\delta$  74.88, 69.12, 32.54, 29.49, 29.07, 26.80, 25.91 ppm.

Synthesis of Polybromohydrin (pBrOH). A 20 mL scintillation vial was charged with a stir bar and epoxidized PCOE (0.25 g, 0.0085 mmol). The polymer was dissolved in 10 mL of THF on a magnetic stir plate. Once dissolved, HBr (4.7 mL, 42 mmol) was added dropwise to the polymer solution. After 18 h, the solution was removed from the stir plate and precipitated dropwise in a 10-fold excess by volume stirred deionized water. Sodium bicarbonate (5.25 g, 62 mmol) was added to the solution until a pH strip read as neutral. The solution was left to stir for 6 h to allow the polymer to collect on the stir bar and sides of the beaker. The polymer was collected by decanting off the water and dried overnight in the vacuum oven at 50  $^{\circ}$ C. The percent yield was 99%.  $M_{\rm n,NMR} = 14\,600$  g/mol;  $^{1}$ H NMR (500 MHz, CDCl<sub>3</sub>)  $\delta$  4.23–4.13 (m, 1nH), 4.11–4.03 (m, 1nH), 3.74-3.64 (m, 1nH), 3.54-3.45 (m, 1nH), 2.18-1.19 (m, 12nH), 1.15-1.08 (t, 6H), 1.06-1.01 (t, 6H) ppm; <sup>13</sup>C NMR (400 MHz,  $CDCl_3$ )  $\delta$  74.94, 65.20, 35.77, 33.22, 30.42, 29.52, 28.96, 27.94, 25.91, 25.69 ppm.

Synthesis of Polyiodohydrin (pIOH). A 20 mL scintillation vial was charged with a stir bar and epoxidized PCOE (0.25 g, 0.0085 mmol). The polymer was dissolved in 10 mL of THF on a magnetic stir plate. Once dissolved, HI (5.6 mL, 42 mmol) was added dropwise to the polymer solution. After 18 h, the solution was removed from the stir plate and precipitated dropwise in a 10-fold excess by volume stirred DI water. Sodium bicarbonate (3.5 g, 42 mmol) was added to the solution until a pH strip read as neutral. The polymer stuck to the stir bar and was collected by decanting off the water and removing the polymer. The polymer was redissolved in THF and reprecipitated in a 10-fold excess by volume of stirred deionized water with L-ascorbic acid (1.0 g, 5.6 mmol). The polymer was left stirring to collect on the stir bar, followed by decanting and removing the polymer. The polymer was dried overnight in the vacuum oven at room temperature. The polymer following collection was bright yellow in color. The percentage yield was 83%.  $M_{n,NMR} = 46\,900$  g/mol; <sup>1</sup>H **NMR** (500 MHz, CDCl<sub>3</sub>)  $\delta$  5.46–5.33 (m, 2nH), 4.37–4.27 (m, 1nH), 4.24-4.15 (m, 1nH), 3.38-3.28 (m, 1nH), 2.94-2.85 (m, 1nH), 2.11-1.94 (m, 4nH), 1.93-1.21 (m, 12nH), 1.10-1.06 (t, 6H), 1.06-1.02 (t, 6H), 1.00-0.96 (t, 6H) ppm.

**Chemical Characterization.** Proton nuclear magnetic resonance ( $^{1}$ H NMR) spectra were recorded on a Fourier transform NMR spectrometer at 298 K at 500 MHz. Chemical shifts are reported relative to the solvent resonance peak (CDCl<sub>3</sub>:  $\delta$  = 7.26 ppm) for  $^{1}$ H NMR spectra.  $^{1}$ H NMR of PCOE, epoxidized PCOE (epoxPCOE), and all polyhalohydrins were conducted in 5 mm diameter NMR tubes on a Bruker 500 MHz spectrometer.  $^{1}$ H NMR was performed with 16 scans and a d1 relaxation time of 5 s in deuterated chloroform (CDCl<sub>3</sub>). Carbon nuclear magnetic resonance ( $^{13}$ C NMR) spectra were recorded on a Fourier transform NMR spectrometer at 298 K and 400 MHz. Chemical shifts are reported relative to the solvent resonance peak (CDCl<sub>3</sub>:  $\delta$  = 77.16 ppm). Fourier-Transform Infrared

Spectroscopy (FTIR) analyses were performed using a Nicolet iS50 FTIR spectrometer equipped with an attenuated total reflectance (ATR) module. The polymer samples, after drying under vacuum at 50 °C overnight, were compressed against a diamond ATR crystal using an anvil. ATR-FTIR spectra were recorded with a spectral resolution of 0.2 cm<sup>-1</sup>, and each spectrum was obtained by averaging 100 scans.

**Thermal Characterization.** Thermogravimetric analysis (TGA) was performed using a TA Instruments Q50 thermal gravimetric analyzer. Approximately 10 mg of polymer was loaded onto a platinum TGA pan. Samples were first equilibrated at 25 °C before heating to 500 °C at a rate of 10 K/min. Differential scanning calorimetry (DSC) was performed using a TA Q2000 instrument with  $\sim\!5-10$  mg of polymer loaded into hermetic aluminum pans. Samples were initially cooled to -50 °C followed by heating to  $\sim\!5$  °C below  $T_{\rm d,1.5\%}$  to erase thermal history.  $T_{\rm d,1.5\%}$  is the temperature at which the sample has experienced a degradative mass loss of 1.5% as measured during TGA. The sample was then cooled to -50 °C, and subsequently heated  $\sim\!5$  °C below  $T_{\rm d,1.5\%}$ . The heating and cooling rates are 10 K/min.

Lap Joint Shear. The adhesive performance of polyhalohydrins was evaluated using lap joint shear tests (ASTM D1002) with five replicates per polymer. Polymer solutions (23 wt % in THF) were homogenized via vortex mixing (~15 min, Fisher Scientific) and degassed overnight at room temperature. The degassed solutions were then blade-coated onto aluminum (Al) coupons using a 100 mm-wide micrometer-adjustable film applicator mounted on a blade coater (MSK-AFA-III-HB) at a traverse speed of 6 mm/min. Coated coupons were kept in a fume hood overnight, followed by heating on a covered hot plate at 60 °C for 1 h to remove residual solvent. Two aluminum coupons were brought into contact at their coated ends, secured using binder clips, and thermally treated in a vacuum oven for 30 min at 90 °C for pClOH and pBrOH, and at 70 °C for pIOH. Lap shear tests were performed using an Instron tabletop universal testing machine (Model 5564, Merlin Series IX) at a strain rate of 1.5 mm/ min with a 2 kN load cell. After joint failure, the bonded overlap area was measured using digital calipers. Ultimate shear stress was calculated by dividing the maximum applied force by the bonded area.

Contact Angle and Surface Free Energy. Wettability and surface free energy were assessed at room temperature using a Ramé-Hart Model 250-U4 goniometer. The sessile drop method was employed, and the contact angle between the film surface and the droplet's tangent was analyzed using DROPimage Advanced software. For each polymer, three independently prepared films were tested, with contact angles values averaged over 15–18 measurements. Polyhalohydrin films were prepared using the same procedure as for lap joint shear tests, except that they were cast onto Tefzel substrates. Solvent removal was carried out in two steps: overnight in a loosely covered container in a fume hood, followed by stepwise heating (10–20 K/h) on a covered hot plate to minimize bubble formation. pClOH and pBrOH films were heated from 50 to 110 °C, while pIOH films were heated from 50 to 80 °C. Fully hydrogenated PCOE (h-PCOE) films were hot-pressed at 130 °C using a Carver press with

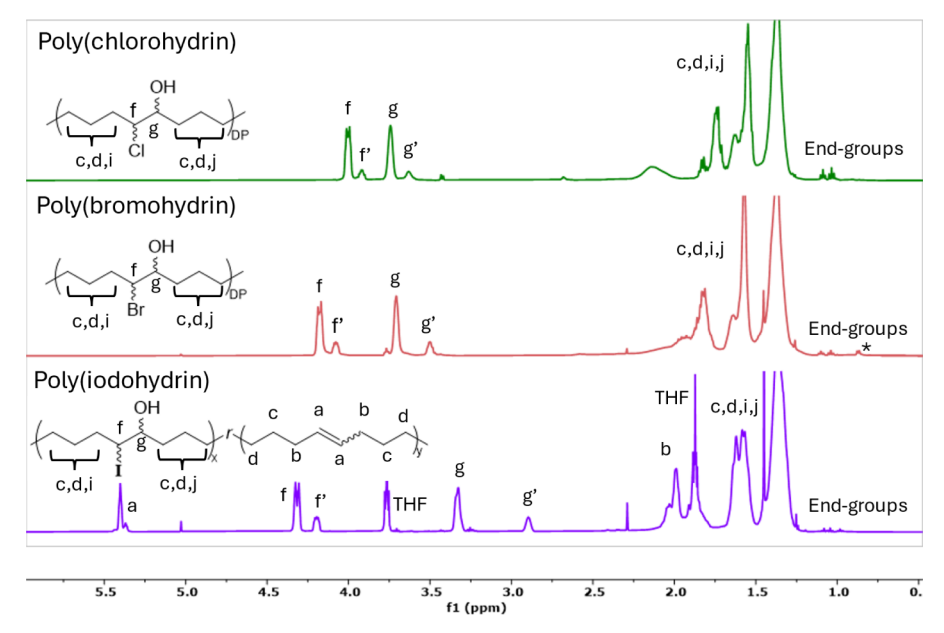


Figure 2. <sup>1</sup>H NMR of polychlorohydrin (top), polybromohydrin (middle), and polyiodohydrin (bottom). The \* at  $\delta$  0.9 ppm of the poly(bromohydrin) is identified as silicone grease.

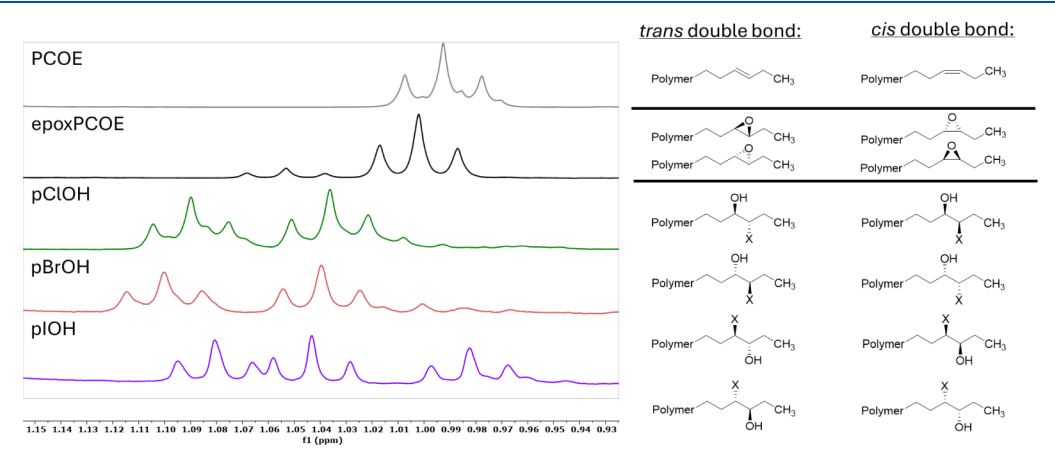


Figure 3. <sup>1</sup>H NMR chemical shifts of methyl end-groups from the *cis*-3-hexene chain-transfer agent are sensitive to the nearest neighbor functionality.

PTFE liners inside steel window plates. The samples were pressed at 1.5 tons for 10 min, then cooled to room temperature between the plates.

For water contact angle (WCA) measurements, 4–9  $\mu$ L droplets of ultrapure deionized water (UDI, Milli-Q, 18.2 M $\Omega$ ·cm) were placed on the films and imaged within 15 s of placement. Surface free energy (SFE) values were calculated using contact angles of high-polarity UDI H<sub>2</sub>O and high-dispersion CH<sub>2</sub>I<sub>2</sub>, with separate syringes used to prevent cross-contamination. Polar and dispersive SFE components were determined using Young's eq eq 1 and Wu's harmonic-mean eq eq 2.  $^{30,31}$ 

$$\gamma_{\rm s} - \gamma_{\rm sl} = \gamma_{\rm l} \cos(\theta) \tag{1}$$

$$\gamma_{sl} = \gamma_s + \gamma_l - 4 \left( \frac{\gamma_s^d \times \gamma_l^d}{\gamma_s^d + \gamma_l^d} + \frac{\gamma_s^P \times \gamma_l^P}{\gamma_s^P + \gamma_l^P} \right)$$
 (2)

where  $\theta$  is the contact angle,  $\gamma_s$ ,  $\gamma_l$  and  $\gamma_{sl}$  represent the solid surface free energy, liquid surface tension, and solid—liquid interfacial energy (mJ/m²), respectively. The terms  $\gamma_s^P$  and  $\gamma_s^d$  are the polar and dispersive components of the solid's surface energy, respectively, and  $\gamma_s^P$  and  $\gamma_s^d$  are those of the liquid. Total SFE was calculated as the sum

of polar and dispersive components. The standard deviation of the contact angle was used to propagate uncertainty in SFE through a Python package for calculations with uncertainties.<sup>32</sup>

# ■ RESULTS AND DISCUSSION

Synthesis and Chemical Characterization of Polyhalohydrins. Fully epoxidized polycyclooctene (epoxPCOE) was successfully ring-opened with HCl, HBr, or HI to generate the respective polyhalohydrins, Scheme 1. Halohydrin synthesis was performed on a single batch of epoxPCOE, allowing for a direct comparison between the reactions and the resulting polymers. This ring-opening proceeds to 100% conversion with 1.2 equiv of halo acid relative to epoxide, in 18 h of reaction time.

The polymers were characterized by <sup>1</sup>H NMR and there was an absence of any remaining epoxide methine resonances indicating complete conversion, Figure 2. For the polychlorohydrin (pClOH), polybromohydrin (pBrOH), and polyiodohydrin (pIOH) there were four new proton resonances corresponding to the methine protons of the halide and hydroxide functionality (f, f', g, g'). The <sup>1</sup>H NMR spectrum of

PCOE and epoxPCOE (Figures S1 and S2) and full <sup>1</sup>H NMR spectra with integrations (Figures S3, S5 and S7) are found in the Supporting Information.

The polyhalohydrins prepared are both stereoirregular and regioirregular. The halide anion from the inorganic acids acts as a nucleophile and there is equal probability of attacking either carbon of the epoxide. This is contrasted with the symmetry of epoxPCOE in which the epoxide can only be in the trans or cis configuration. In each spectrum there are two major and two minor peaks in the region of  $\delta = 2.8 - 4.5$  ppm, corresponding to the methylylidene protons of the halide and hydroxide functional groups. Integration of the peaks reveals that the ratio of major:minor was 77:23, which matched the integration ratio of trans:cis in the original batch of PCOE as well as the major to minor, trans:cis ratio in the epoxidized polymers. There are, however, a few key differences between the chemical shifts of the peaks in pClOH, pBrOH, and pIOH. Across the series from chloro- to bromo- and iodofunctionality, the halide methine protons exhibit a downfield shift, while the hydroxyl methine protons shift upfield, resulting in greater separation.

The polymers studied have methyl end-groups, stemming from the use of cis-3-hexene as a chain transfer agent in the ring-opening metathesis polymerization of cis-cyclooctene, Scheme S1. It is apparent from the <sup>1</sup>H NMR that the protons of the methyl end-groups have chemical shifts at  $\sim 0.93 - 1.13$ ppm that are sensitive to the nearest functionality, Figures 3 and S9. This sensitivity is simplest to understand in the PCOE, where the nearest functional group is either a cis- or transdouble bond, resulting in two triplets, with nearly identical chemical shifts. When the PCOE has been fully epoxidized, the two end-group triplets have distinct chemical shifts, corresponding to four possible end-groups. The ratio of the integrations of the major to minor triplets is once again consistent with that of the major to minor backbone methine protons. In the case of the polyhalohydrins, the splitting becomes more complex as the number of end-group possibilities increases with the stereoirregularity and regioirregularity. The <sup>1</sup>H NMR of pClOH and pBrOH have four overlapping triplets from the eight end-group possibilities.

There are also peaks in the pIOH <sup>1</sup>H NMR that correspond to vinylic and allylic resonances, indicative of alkenes. We suspect these alkene protons are due to the labile nature of the iodide functional group, resulting in elimination chemistry. 33,34 Of the three halides in this study, carbon-iodine bonds have the lowest bond dissociation energy and the longest bond length.<sup>35</sup> This is supported by early experimental results in which the ring-opening with hydroiodic acid led to insoluble, cross-linked polymers. Additionally, free I2 is present in the solution above the precipitated polymer as evidenced by the dark red/purple color. When attempting to redissolve this polymer, the solution turned a bright pink color, further supporting the hypothesis. The challenges in synthesizing a non-cross-linked polymer were overcome by the addition of ascorbic acid (vitamin C) as an iodine scavenger. 36,37 Due to the increased complexity of the polyiodohydrins there are more end-group possibilities.

The polymers were synthesized from a single batch of PCOE that had 100% of the double bonds epoxidized. Control experiments were performed to investigate whether there was the potential for the acids to add across double bonds in the backbone, as would be found in PCOE. With all three acids, <sup>1</sup>H NMR of the PCOE before and after treatment showed no

change in the peak integrations and therefore no H-X functionalization of the double bonds, Figures S10–S12. These control experiments have future implications for synthesizing polymers with less than 25 mol % halohydrin and possible orthogonal functionalization, potentially opening the door for increased ability to tailor macroscopic polymer properties.

**Thermal Characterization.** The PCOE, epoxPCOE, and polyhalohydrins were analyzed using differential scanning calorimetry (DSC) and thermogravimetric analysis (TGA). The thermal transition and degradation temperatures are summarized in Table S1. The PCOE and epoxPCOE exhibit 5 wt % degradation ( $T_{\rm d,5\%}$ ) at 379.0 and 298.5 °C, respectively, during a 10 K/min thermal scan under N<sub>2</sub>, Figure S14. In contrast, polyhalohydrins undergo multistage degradation ending with significant mass loss at ~400 °C associated with breaking of C–C backbone bonds. The lower-temperature degradation mechanism (observed at 226.0, 183.9, and 115.6 °C for pClOH, pBrOH and pIOH, respectively) can proceed via two potential pathways, initiated by proton abstraction and the loss of HX, Figure 4. The first pathway involves the

**Figure 4.** Two degradation pathways of polyhalohydrins involve abstraction of a proton from a secondary C–H followed by dehydration to form two double bonds (left) or abstraction of a proton from a tertiary C–H followed by tautomerization to form a ketone (right).

abstraction of a tertiary proton and halide elimination to form a vinyl alcohol intermediate, while the second pathway entails the abstraction of a secondary proton and the halide to form an allylic alcohol intermediate. Further dehydration from the allylic alcohol would result in a second mass loss event, whereas tertiary proton abstraction followed by tautomerization of the vinyl alcohol intermediate results in the formation of a ketone without further mass loss.

To further investigate degradation pathways, we characterized the polymers with FTIR after heating them above the various degradation stages observed in TGA, Figure 5. The polymer samples were thermally treated in the TGA under an inert  $N_2$  atmosphere by heating to the designated temperatures of 300 °C for pClOH, 225 or 300 °C for pBrOH, and 130 or 300 °C for pIOH, followed by cooling to room temperature under  $N_2$ . Post-thermal treatment, FTIR analysis of the samples revealed characteristic absorption bands corresponding to ketone functionalities in all three samples ( $\sim 1700 \text{ cm}^{-1}$ , shown with the arrow in Figure 5), indicating the formation of carbonyl groups during degradation. Furthermore, the mass loss in pClOH and pBrOH above 300 °C falls between the

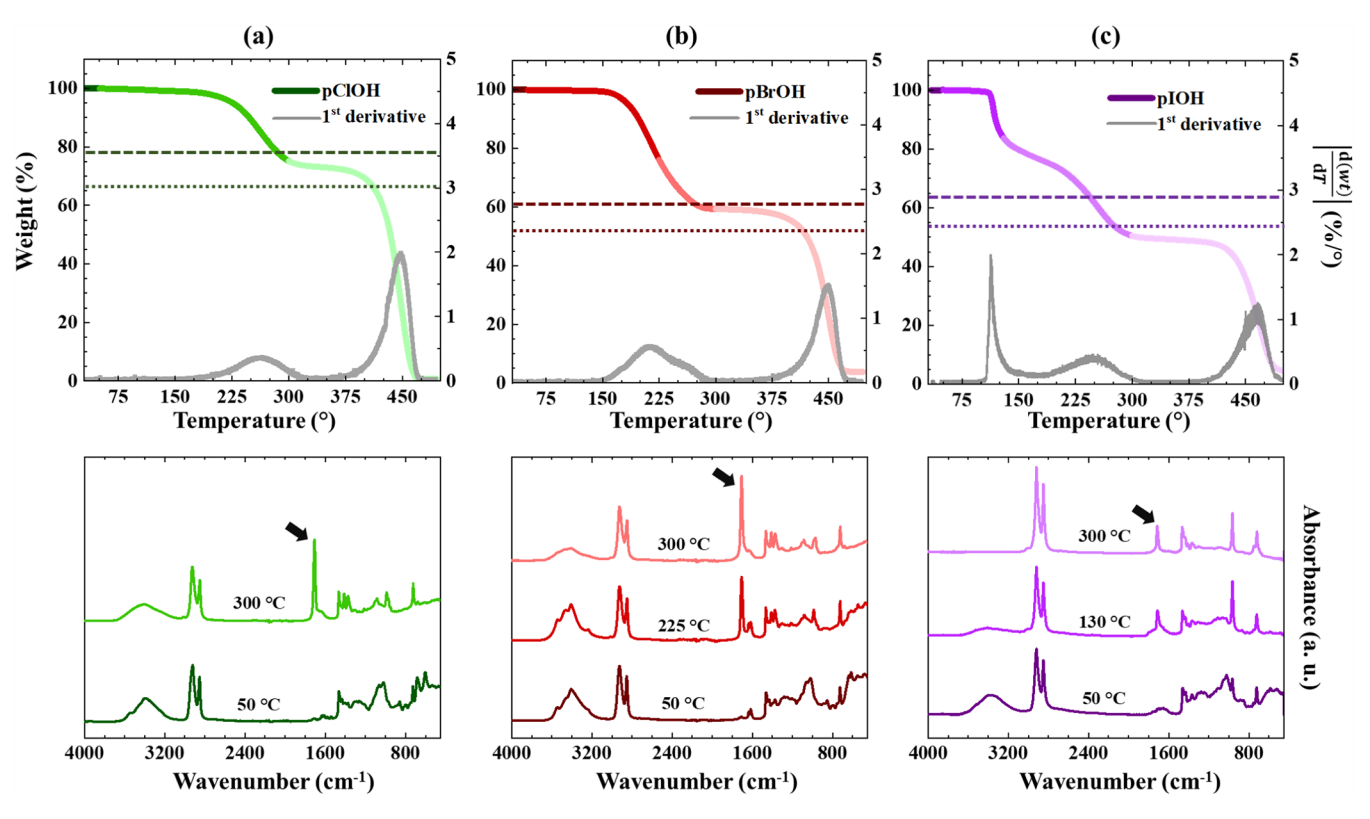


Figure 5. TGA (top) and FTIR (bottom) data for (a) polychlorohydrin (pClOH, green), (b) polybromohydrin (pBrOH, red), and (c) polyiodohydrin (pIOH, purple). TGA thermograms show polymer mass loss (colored lines) and the absolute derivative of mass loss with respect to temperature (gray lines). The predicted weight loss percentages after loss of HX and HX +  $H_2O$  are shown as dashed and dotted lines, respectively. The hues in the TGA profiles correspond to decomposition events, with FTIR spectra collected after the samples had been heated to the select temperatures (e.g., 50  $^{\circ}$ C, 225  $^{\circ}$ C, or 300  $^{\circ}$ C). For all polymers, a carbonyl stretch ( $\sim$ 1700 cm $^{-1}$ ) appears after heating.

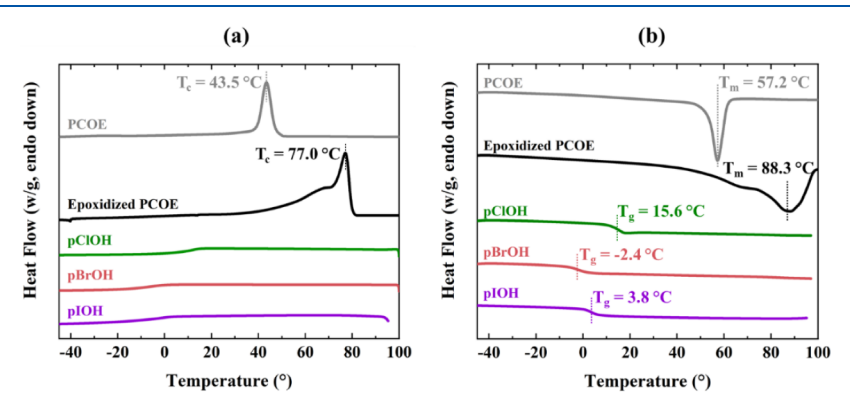


Figure 6. (a) First cooling and (b) second heating DSC curves for polycyclooctene (PCOE, gray), epoxidized PCOE (black), polychlorohydrin (pClOH, green), polybromohydrin (pBrOH, red), and polyiodohydrin (pIOH, purple).

predicted weight loss percentages for the loss of HX and HX + H<sub>2</sub>O, consistent with ketone formation. The mass loss for pIOH is more complicated to interpret due to the presence of alkenes prior to the TGA experiment (Figure 2). Though it occurs at a lower temperature than in the other two halohydrins, the first mass loss event in the TGA curve of pIOH is attributed to the loss of HX. When comparing the bond length and bond strength of a C–I bond to a C–Cl bond or C–Br bond, the C–I bond is both weaker and longer due to the ionic radius of the iodine atom. This decreased bond dissociation energy means that it takes less energy to break the bond compared to the other two halogens, leading to the steepness and lower temperature of the event. Additionally, the shallowness can be attributed to the fact that every repeat unit

no longer represents one halohydrin, with the conversion to the alkene. Overall, ketone formation indicates that the degradation is proceeding via proton abstraction of the tertiary C–H, halide loss, and tautomerization of the vinyl alcohol intermediate to the ketone.

Analysis by DSC and X-ray scattering confirms the amorphous nature of polyhalohydrins, Figures 6 and 7. Measurements by DSC determined the glass transition temperatures ( $T_{\rm g}$ ) as 15.6 °C for pClOH, -2.4 °C for pBrOH, and 3.8 °C for pIOH. The amorphous structure of these polymers is evidenced by the amorphous scattering peak at ~1.4 Å<sup>-1</sup>. The absence of crystallinity is attributed to the presence of stereoirregular and regioirregular halohydrin

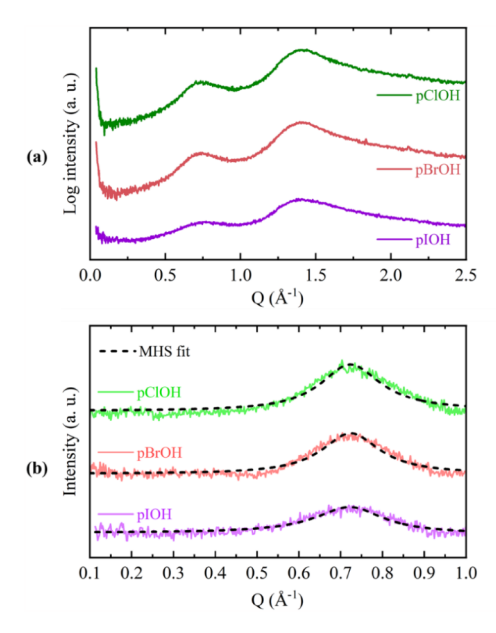
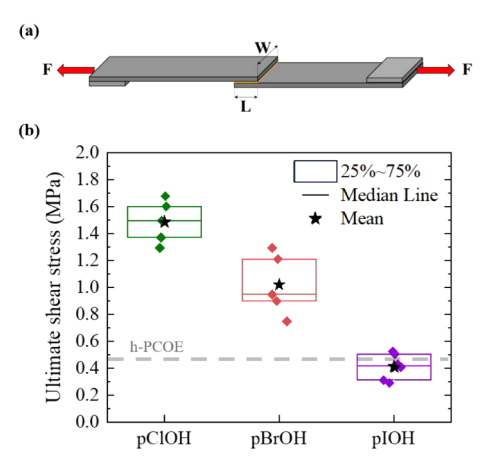


Figure 7. (a) X-ray scattering intensity profiles of polychlorohydrin (pClOH), polybromohydrin (pBrOH), and polyiodohydrin (pIOH) plotted on a logarithmic scale versus the scattering vector Q ( $\mathring{A}^{-1}$ ). (b) Aggregate peak fit by the modified hard-sphere scattering model (MHS, black dashed lines) across the q-range of 0.1–1  $\mathring{A}^{-1}$ .

functional groups that disrupt molecular packing and prohibit crystal formation.

In addition to the amorphous halo associated with the backbones, there is an additional broad scattering associated with interaggregate scattering from the functional groups, which we attribute to clustering of halohydrin groups driven by hydrogen and halogen bonding within the nonpolar backbone matrix. Scattering intensity in the q-range  $0.1-1 \text{ Å}^{-1}$  was baseline-subtracted and fit with the modified hard-sphere (MHS) model to extract information about the aggregate morphology (eqs S1-S3 and further details). 39,40 The MHS model assumes monodisperse spheres distributed throughout the matrix with a minimum separation (radius of closest approach) and fits the X-ray scattering data well; see Figure 7. The radii of aggregates found by the MHS model are 2.37 Å for pClOH, 2.79 Å for pBrOH, and 2.94 Å for pIOH (Table S2). By comparing the volume of these aggregates with the estimated volume of the functional groups, the aggregates appear to contain 2 to 3 halohydrin groups, namely dimers and trimers. We acknowledge that while a good fit between the data and the MHS alone is insufficient to definitively claim the presence of spherical aggregates, the peak at  $\sim 0.7 \text{ Å}^{-1}$  clearing indicated the assembly of functional group in these polyhalohydrins. The formation of aggregates will have interesting ramifications on the dynamic mechanical properties of these polymers, and such an investigation is left for future

Adhesive Properties and Surface Free Energy. Lap joint shear experiments assessed the adhesive properties of the polyhalohydrins. A schematic of the loading configuration is presented in Figure 8a. Among the polyhalohydrins, pClOH exhibits the highest ultimate shear stress  $(1.5 \pm 0.2 \text{ MPa})$ , followed by pBrOH  $(1.0 \pm 0.2 \text{ MPa})$ , while pIOH exhibits the lowest  $(0.4 \pm 0.1 \text{ MPa})$ , Figures 8b and S15. Notably, the ultimate shear stress of pClOH is nearly three times that of the hydrogenated PCOE  $(0.48 \pm 0.15 \text{ MPa})$ . The observed



**Figure 8.** (a) Schematic of the single lap joint shear test configuration. (b) Ultimate shear stress for polyhalohydrins and h-PCOE. <sup>41</sup> Note that all samples exhibited mixed adhesive and cohesive failure modes. The box plot indicates the interquartile range (25th to 75th percentiles), with the median represented by the central line and the mean by a star. An increasing trend in ultimate shear stress is observed in the order of pIOH < pBrOH < pCIOH.

trend is attributed to interfacial interactions between the hydroxyl and halogen functionalities in the polymers and the aluminum hydroxide surface layer that naturally forms upon exposure of aluminum to air.  $^{42}$  Furthermore, adhesion is likely enhanced by polar interactions between the halogen atoms and the polar aluminum hydroxide surface. The relative adhesive strengths correlate with the electronegativity of the halogens (Cl > Br > I), as more electronegative halogens induce stronger dipole interactions with the polar substrate.

Wettability and surface energy of the polyhalohydrins and hydrogenated PCOE (h-PCOE), a model for HDPE, were evaluated using contact angle measurements and surface free energy (SFE) calculations, Figures 9 and S16. The average water contact angles (WCA) are  $79.3^{\circ} \pm 2.4^{\circ}$  for pClOH,  $86.2^{\circ} \pm 2.3^{\circ}$  for pBrOH, and  $94.3^{\circ} \pm 4.4^{\circ}$  for pIOH. A paired t test confirmed that the differences in WCA between the polyhalohydrins are statistically significant (p-value < 0.05), demonstrating a clear impact of halohydrin functionality on surface wettability (Tables S3-S5). Both pClOH and pBrOH exhibit lower WCAs compared to commercial HDPE (~95- $100^{\circ}$ ) and h-PCOE (92.0°  $\pm$  2.7°). The presence of polar hydroxyl and halogen functional groups clearly lower the WCA, as expected.<sup>43–48</sup> The somewhat higher WCA and greater standard deviation observed for pIOH are attributed to the partial reversion of iodohydrins to alkenes, introducing backbone unsaturation as detailed above. This unsaturation lowers the surface density of polar functional groups, resulting in decreased hydrophilicity. In addition, iodine's lower electronegativity reduces the polarity of the C-I bond, and its larger atomic radius can sterically shield neighboring hydroxyl groups, limiting interaction with water, both factors contributing to lower wettability compared to bromo- and chlorohydrin. The WCA values of the pClOH and pBrOH are comparable to those of poly(ethylene-co-vinyl alcohol) with 56 mol % hydroxyl groups (WCA 76-85°), 5,49,50 and indicate greater wettability than 36% chlorinated polyethylene (WCA ~92°).51,52

The Wu method was employed to separate the surface free energy (SFE) into polar and dispersive components. The SFE measurements indicate that pClOH exhibits the highest

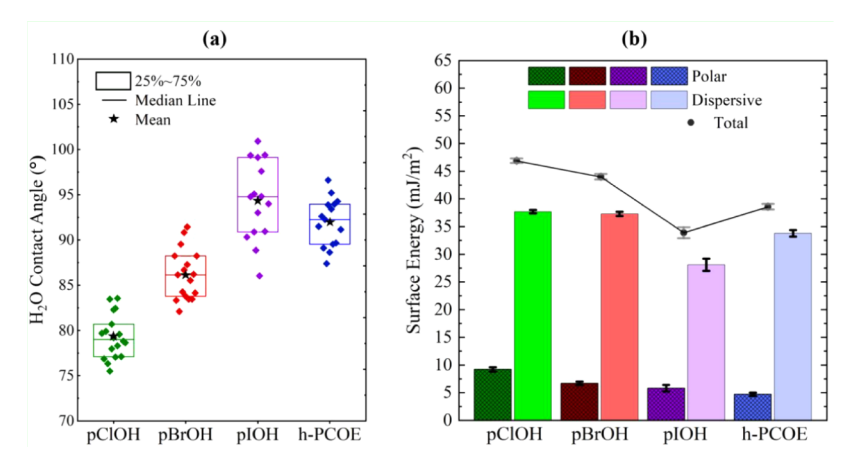


**Figure 9.** (a) Water contact angle measurements for polyhalohydrin films and hydrogenated PCOE (h-PCOE), where the box represents the 25th to 75th percentiles, the median is shown as a line, and the mean is marked with a star. A trend of decreasing water contact angle is observed, indicating that the polymers become increasingly hydrophilic in the order of pIOH < pBrOH < pCIOH. (b) Surface free energy components of the films, where polar components (darker shades) and dispersive components (lighter shades) reveal a similar trend. Total surface free energy shown by symbols.

total surface energy ( $\gamma_{pCIOH}$  = 46.8  $\pm$  0.4 mJ/m²), followed by pBrOH ( $\gamma_{pBrOH}$  = 44.0  $\pm$  0.5 mJ/m²) and pIOH ( $\gamma_{plOH}$  = 33.9  $\pm$  1.0 mJ/m²), Figure 9b. Similarly, the polar component is highest for pClOH ( $\gamma_{pClOH}^p$  = 9.2  $\pm$  0.4 mJ/m<sup>2</sup>), followed by pBrOH ( $\gamma_{\rm pBrOH}^{\rm p}$  = 6.7  $\pm$  0.3 mJ/m²), and pIOH ( $\gamma_{\rm pIOH}^{\rm p}$  = 5.8  $\pm$ 0.4 mJ/m<sup>2</sup>). Compared to h-PCOE ( $\gamma_{h-PCOE}^{p} = 4.7 \pm 0.3$  mJ/ m<sup>2</sup>), the polar component of surface energy increases by 95.7%, 42.6%, and 23.4% for pClOH, pBrOH, and pIOH, respectively. This increase is attributed to the intrinsic polarity of the hydroxyl group and the effect of halogen electronegativity on dipole strength. Chlorine, being more electronegative than bromine and iodine, forms a stronger C-Cl dipole, increasing the overall polarity of pClOH. Consequently, pClOH shows the highest polar component of surface energy among the polyhalohydrins. In contrast, the lower electronegativities of bromine and iodine result in weaker dipoles in pBrOH and pIOH, leading to smaller increases in polar surface energy.

In contrast, the dispersive component shows only modest variation. Both pClOH and pBrOH show slightly higher dispersive components ( $\gamma_{\rm pClOH}^{\rm d}$  = 37.7  $\pm$  0.3 mJ/m<sup>2</sup> and  $\gamma_{\rm pBrOH}^{\rm d}$ = 37.3  $\pm$  0.4 mJ/m²) compared to h-PCOE ( $\gamma_{h-PCOE}^{d}$  = 33.8  $\pm$ 0.6 mJ/m<sup>2</sup>), corresponding to increases of 11.5% and 10.3%, respectively. This increase may be attributed to the greater polarizability of Cl and Br atoms compared to the fully hydrocarbon-based h-PCOE.<sup>54</sup> pIOH has the lowest dispersive component ( $\gamma_{\rm pIOH}^{\rm d}$  = 28.1  $\pm$  1.1 mJ/m<sup>2</sup>) consistent with the reversion of iodohydrin groups to alkenes. During this process, some halohydrin groups are eliminated and replaced with C= C bonds, resulting in a lower mol % of halogen-containing moieties and leading to a decrease in the overall dispersive component of SFE. The lower dispersive component of pIOH compared to h-PCOE may also be influenced by its amorphous morphology, as reduced crystallinity can diminish the density of dispersive interactions at the surface.<sup>55</sup>

The adhesion strength of the polyhalohydrins and h-PCOE, as measured via single lap shear testing, reveals a clear increasing trend with total surface energy, Figure 10. The higher surface energy of pClOH, indicates stronger inter-

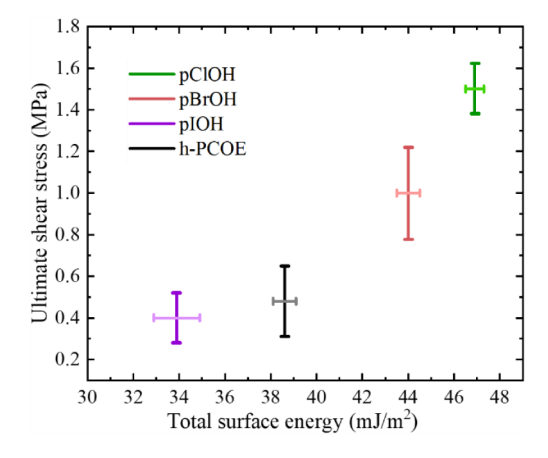


**Figure 10.** Ultimate shear stress versus total surface energy for polyhalohydrins and h-PCOE, showing a positive correlation between surface energy and lap joint adhesive strength.

actions at the adhesive-substrate (aluminum coupon) interface, contributing to its improved adhesion performance compared to pBrOH and pIOH. This positive correlation is well supported in literature. For example, Starostina et al. demonstrated that introducing polar amine groups into HDPE enhances adhesion to steel substrates through acid-base and donor-acceptor interactions, while the dispersive component remained largely unchanged. 56 They also noted that an excess of polar groups can reduce adhesion strength, potentially due to aggregation, phase separation, or plasticization effects. Thurston et al. similarly observed that increasing the surface energy of low-energy polymers like polyethylene via plasma treatment improved lap shear strength with various adhesives.<sup>57</sup> Thermodynamically, Ghanbari et al. showed that the work of adhesion scales with total surface energy, and surface treatments that increase SFE enhance bonding to polar adhesives. 58 Likewise, Yamauchi et al. highlighted that beyond a critical surface energy threshold (~20 mN/m), adhesion becomes strongly surface energy-dependent.<sup>59</sup> Finally, Smith emphasized that increased polar surface energy correlates with higher shear strength in lap joints, consistent with the performance difference between the polymers in our study.

These results suggest that halohydrin-functionalized polyolefins offer a chemically tunable platform to control interfacial properties by modifying the polar surface energy. The ability to vary halohydrin type and functional group density, along with the option for orthogonal functionalization, creates opportunities to tailor macroscopic properties. Systematic exploration across various halohydrin functional group densities and additional physical properties could further broaden the utility of this approach.

## CONCLUSION

The synthesis of halohydrin-functionalized polycyclooctene (PCOE) was successfully achieved through a two-step process involving epoxidation followed by epoxide ring-opening with HCl, HBr, or HI. The resulting polymers, polychlorohydrin (pClOH), polybromohydrin (pBrOH), and polyiodohydrin (pIOH) were characterized to assess their structural and adhesive properties. Control experiments showed no reaction between the double bonds of the PCOE and the acids under the conditions utilized, introducing potential for further tunability of functionality.

Differential scanning calorimetry and X-ray scattering measurements found that the polyhalohydrins exhibit amorphous morphologies, contrasted with the semicrystalline nature of the PCOE and epoxPCOE. This absence of crystallinity is attributed to the stereoirregular and regioirregular incorporation of halohydrin functional groups, which disrupt molecular packing and hinder orderly structure formation. X-ray scattering also provides evidence of the halohydrin functional groups forming dimers and trimers.

Lap joint shear testing demonstrated improved adhesion with halohydrin functionalization, with ultimate shear stress following the order: pClOH (1.5  $\pm$  0.2 mJ/m<sup>2</sup> > pBrOH (1.0  $\pm 0.2 \text{ mJ/m}^2 > \text{pIOH } (0.4 \pm 0.1 \text{ mJ/m}^2)$ . Notably, pClOH achieved nearly a 3-fold increase in shear strength over hydrogenated PCOE, linked to enhanced interfacial interactions via polar functionalities. Contact angle and surface energy analysis further confirmed a rise in polarity across the series, mirroring the observed adhesion trends and reinforcing the role of polar surface energy in interfacial bonding. These findings support halohydrin functionalization as a versatile strategy for tuning regiointerfacial properties of polyolefins. Overall, this study expands the toolbox for chemical modification of polyolefins, offering a platform for designing materials with tailored macroscopic behaviors, such as adhesion, through controlled introduction of reactive and orthogonally accessible functional groups.

## ASSOCIATED CONTENT

# Supporting Information

The Supporting Information is available free of charge at https://pubs.acs.org/doi/10.1021/acs.macromol.5c01830.

Materials; polycyclooctene (PCOE) synthesis; epoxidized polycyclooctene synthesis; hydrochloric, hydrobromic and hydroiodic acid control experiments; NMR spectra along with end group analysis; thermogravimetric analysis; X-ray scattering method and analysis; lap joint shear data; water contact angle data and analysis (PDF)

#### AUTHOR INFORMATION

# **Corresponding Authors**

Karen I. Winey — Department of Materials Science and Engineering, University of Pennsylvania, Philadelphia, Pennsylvania 19104, United States; Department of Chemical and Biomolecular Engineering, University of Pennsylvania, Philadelphia, Pennsylvania 19104, United States; orcid.org/0000-0001-5856-3410; Email: Winey@seas.upenn.edu

E. Bryan Coughlin – Department of Polymer Science and Engineering, University of Massachusetts Amherst, Amherst, Massachusetts 01003, United States; orcid.org/0000-0001-7065-4366; Email: ebc@umass.edu

#### **Authors**

Anne N. Radzanowski – Department of Polymer Science and Engineering, University of Massachusetts Amherst, Amherst, Massachusetts 01003, United States; orcid.org/0000-0001-6453-3103

Hoda Shokrollahzadeh Behbahani – Department of Materials Science and Engineering, University of Pennsylvania, Philadelphia, Pennsylvania 19104, United States

William McCambridge – Department of Materials Science and Engineering, University of Pennsylvania, Philadelphia, Pennsylvania 19104, United States; orcid.org/0009-0006-3150-6807

Clay Gensel — Department of Polymer Science and Engineering, University of Massachusetts Amherst, Amherst, Massachusetts 01003, United States

Catherine Spence – Department of Polymer Science and Engineering, University of Massachusetts Amherst, Amherst, Massachusetts 01003, United States

Complete contact information is available at: https://pubs.acs.org/10.1021/acs.macromol.5c01830

## **Author Contributions**

\*A.N.R. and H.S.B. contributed equally.

#### Notes

The authors declare no competing financial interest.

# ACKNOWLEDGMENTS

The authors gratefully acknowledge funding by DOE BES (DESC0022238). The authors also wish to acknowledge Eli Fastow for his assistance with X-ray scattering. H.S.B. and K.I.W. acknowledge the use of the Dual Source and Environmental X-ray Scattering facility operated by the Laboratory for Research on the Structure of Matter at the University of Pennsylvania supported by the NSF through the DMR-2309043 grant.

## REFERENCES

- (1) Hiemenz, P.; Lodge, T. Polymer Chemistry, 2nd ed.; CRC Press: New York, 2007.
- (2) Dingwell, C. E.; Hillmyer, M. A. Regio- and Stereoregular EVOH Copolymers from ROMP as Designer Barrier Materials. *ACS Polym. Au* **2024**, *4* (3), 208–213.
- (3) Maes, C.; Luyten, W.; Herremans, G.; Peeters, R.; Carleer, R.; Buntinx, M. Recent Updates on the Barrier Properties of Ethylene Vinyl Alcohol Copolymer (EVOH): A Review. *Polym. Rev* **2018**, *58* (2), 209–246.
- (4) Kuraray. Kuraray EVAL<sup>TM</sup> EVOH-Kuraray. https://eval.kuraray.com/. (Accessed 17 september 2023).

- (5) Tenn, N.; Follain, N.; Fatyeyeva, K.; Valleton, J.-M.; Poncin-Epaillard, F.; Delpouve, N.; Marais, S. Improvement of Water Barrier Properties of Poly(Ethylene- *Co* -Vinyl Alcohol) Films by Hydrophobic Plasma Surface Treatments. *J. Phys. Chem. C* **2012**, *116* (23), 12599–12612.
- (6) Jimenez Antenucci, P. M.; Radzanowski, A. N.; Fastow, E. J.; Votruba-Drzal, J.; Redder, M.; Winey, K. I.; Coughlin, E. B.; Kozlowski, M. C. Synthesis and Blending of Two Poly(Ethylene-Co-Vinyl Alcohol) Polymers with Mixed 1,2-Diol Stereochemistry. *ACS Appl. Polym. Mater* **2025**, 7 (11), 7275–7282.
- (7) Zhang, H.; Zhou, L. Evaluation of Performance of Chlorinated Polyethylene Using Wireless Network and Artificial Intelligence Technology. *Wirel. Commun. Mob. Comput* **2022**, 2022 (1), 7261207.
- (8) Bogert, M. T.; Slocum, E. M. The Preparation Of Various Aliphatic Halides And Halohydrin Compounds. *J. Am. Chem. Soc* **1924**, *46* (3), 763–768.
- (9) Lin, H.; Chen, Y.-Z.; Xu, X.-Y.; Xia, S.-W.; Wang, L.-X. Preparation of Key Intermediates of Adrenergic Receptor Agonists: Highly Enantioselective Production of (*R*)-α-Halohydrins with Saccharomyces Cerevisiae CGMCC 2.396. J. Mol. Catal. B: Enzym 2009, 57 (1), 1–5.
- (10) Parker, R. E.; Isaacs, N. S. Mechanisms Of Epoxide Reactions. *Chem. Rev* **1959**, *59* (4), 737–799.
- (11) Thirumalaikumar, M. Ring Opening Reactions of Epoxides. A Review. *Org. Prep. Proced. Int* **2022**, *54* (1), 1–39.
- (12) Kim, C.; Traylor, T. G.; Perrin, C. L. MCPBA Epoxidation of Alkenes: Reinvestigation of Correlation between Rate and Ionization Potential. J. Am. Chem. Soc 1998, 120 (37), 9513–9516.
- (13) Lorwanishpaisarn, N.; Sae-Oui, P.; Sirisinha, C.; Siriwong, C. A New Approach to the Epoxidation of Natural Rubber through a Sonochemical Method. *Ind. Crops Prod* **2023**, *197*, 116629.
- (14) Morontsev, A. A.; Denisova, Y. I.; Gringolts, M. L.; Filatova, M. P.; Shandryuk, G. A.; Finkelshtein, E. S.; Kudryavtsev, Y. V. Epoxidation of Multiblock Copolymers of Norbornene and Cyclooctene. *Polym. Sci., Ser. B* **2018**, *60* (5), 688–698.
- (15) Xu, L.; Li, B.-G.; Jie, S.; Li, Z.; Bu, Z. 110th Anniversary: The Epoxidation of Polybutadiene via Reaction-Controlled Phase-Transfer Catalysis. *Ind. Eng. Chem. Res* **2019**, *58* (29), 13085–13092.
- (16) Hussain, H.; Al-Harrasi, A.; Green, I. R.; Ahmed, I.; Abbas, G.; Rehman, N. U. Meta-Chloroperbenzoic Acid (mCPBA): A Versatile Reagent in Organic Synthesis. *RSC Adv* **2014**, 4 (25), 12882–12917.
- (17) Srivastava, V. K.; Basak, G. C.; Maiti, M.; Jasra, R. V. Synthesis and Utilization of Epoxidized Polybutadiene Rubber as an Alternate Compatibilizer in Green-Tire Composites. *Int. J. Ind. Chem* **2017**, 8 (4), 411–424.
- (18) Matic, A.; Hess, A.; Schanzenbach, D.; Schlaad, H. Epoxidized 1,4-Polymyrcene. *Polym. Chem* **2020**, *11* (7), 1364–1368.
- (19) Mehić, E.; Hok, L.; Wang, Q.; Dokli, I.; Miklenić, M. S.; Blažević, Z. F.; Tang, L.; Vianello, R.; Elenkov, M. M. Expanding the Scope of Enantioselective Halohydrin Dehalogenases Group B. Adv. Synth. Catal 2022, 364 (15), 2576—2588.
- (20) Schallmey, A.; Schallmey, M. Recent advances on halohydrin dehalogenases—from enzyme identification to novel biocatalytic applications. *Appl. Microbiol. Biotechnol* **2016**, *100*, 7827–7839.
- (21) Hasnaoui-Dijoux, G.; Elenkov, M. M.; Spelberg, J. H. L.; Hauer, B.; Janssen, D. B. Catalytic Promiscuity of Halohydrin Dehalogenase and its Application in Enantioselective Epoxide Ring Opening. *ChemBiochem* **2008**, *9* (7), 1048–1051.
- (22) Wang, Q.-Q.; Song, J.; Wei, D. Origin of Chemoselectivity of Halohydrin Dehalogenase-Catalyzed Epoxide Ring-Opening Reactions. J. Chem. Inf. Model 2024, 64 (11), 4530–4541.
- (23) Carrá, S.; Santacesaria, E.; Morbidelli, M.; Cavalli, L. Synthesis of Propylene Oxide from Propylene Chlorohydrins—I: Kinetic Aspects of the Process. *Chem. Eng. Sci* 1979, 34 (9), 1123–1132.
- (24) Propylene Oxide. https://products.basf.com/basf/products/global/en/cp/propylene-oxide (Accessed 08 September 2024).
- (25) Peng, C.-C.; Abetz, V. A Simple Pathway toward Quantitative Modification of Polybutadiene: A New Approach to Thermorever-

- sible Cross-Linking Rubber Comprising Supramolecular Hydrogen-Bonding Networks. *Macromolecules* **2005**, 38 (13), 5575–5580.
- (26) Zhang, X.; Sun, G.; Zhang, X. A Novel Thermoplastic Shape Memory Polymer with Solid-State Plasticity Derived from Exchangeable Hydrogen Bonds. *RSC Adv* **2020**, *10* (16), 9387–9395.
- (27) Boyd, T. J.; Schrock, R. R. Sulfonation and Epoxidation of Substituted Polynorbornenes and Construction of Light-Emitting Devices. *Macromolecules* **1999**, 32 (20), 6608–6618.
- (28) Stephens, C. H.; Yang, H.; Islam, M.; Chum, S. P.; Rowan, S. J.; Hiltner, A.; Baer, E. Characterization of Polyethylene with Partially Random Chlorine Substitution. *J. Polym. Sci., Part B: Polym. Phys* **2003**, *41* (17), 2062–2070.
- (29) Yang, H.; Islam, M.; Budde, C.; Rowan, S. J. Ring-Opening Metathesis Polymerization as a Route to Controlled Copolymers of Ethylene and Polar Monomers: Synthesis of Ethylene–Vinyl Chloride-like Copolymers. J. Polym. Sci., Part A: Polym. Chem 2003, 41 (13), 2107–2116.
- (30) Wu, S. Calculation of Interfacial Tension in Polymer Systems. J. Polym. Sci. Part C: Polym. Symp 1971, 34 (1), 19–30.
- (31) Wu, S.; Polymer Interface and Adhesion, 1st ed.; Routledge, 2017. DOI: .
- (32) Lebigot, E. O. Uncertainties: A Python package for calculations with uncertainties. https://pythonhosted.org/uncertainties/
- (33) Goering, H. L.; Espy, H. H. The Iodide Ion-Promoted Dehalogenation of Cis- and Trans1,2-Dihalocyclohexanes1. *J. Am. Chem. Soc* **1955**, 77 (19), 5023–5026.
- (34) Miller, S. I.; Noyes, R. M. Iodide-Ion Catalysis of the Elimination of Iodine from Trans-Diiodoethylene and of the Addition of Iodine to Acetylene1,2. *J. Am. Chem. Soc* **1952**, 74 (13), 3403–3406
- (35) Glockler, G. Carbon-Halogen Bond Energies and Bond Distances. J. Phys. Chem 1959, 63 (6), 828-832.
- (36) Silva, C. R.; Simoni, J. A.; Collins, C. H.; Volpe, P. L. O. Ascorbic Acid as a Standard for Iodometric Titrations. An Analytical Experiment for General Chemistry. *J. Chem. Educ* **1999**, *76* (10), 1421
- (37) Yin, X.; Chen, K.; Cheng, H.; Chen, X.; Feng, S.; Song, Y.; Liang, L. Chemical Stability of Ascorbic Acid Integrated into Commercial Products: A Review on Bioactivity and Delivery Technology. *Antioxidants* **2022**, *11* (1), 153.
- (38) Popov, K. V.; Knyazev, V. D. Initial Stages of the Pyrolysis of Polyethylene. *J. Phys. Chem. A* **2015**, *119* (49), 11737–11760.
- (39) Yarusso, D. J.; Cooper, S. L. Analysis of SAXS Data from Ionomer Systems. *Polymer* **1985**, *26* (3), 371–378.
- (40) Buitrago, C. F.; Bolintineanu, D. S.; Seitz, M. E.; Opper, K. L.; Wagener, K. B.; Stevens, M. J.; Frischknecht, A. L.; Winey, K. I. Direct Comparisons of X-Ray Scattering and Atomistic Molecular Dynamics Simulations for Precise Acid Copolymers and Ionomers. *Macromolecules* **2015**, 48 (4), 1210–1220.
- (41) Chethalen, R. J.; Fastow, E. J.; Coughlin, E. B.; Winey, K. I. Thiol–Ene Click Chemistry Incorporates Hydroxyl Functionality on Polycyclooctene to Tune Properties. *ACS Macro Lett* **2023**, *12* (1), 107–112.
- (42) McCafferty, E.; Wightman, J. P. Determination of the Concentration of Surface Hydroxyl Groups on Metal Oxide Films by a Quantitative XPS Method. *Surf. Interface Anal* **1998**, 26 (8), 549–564.
- (43) Bîrleanu, E.; Mihăilă, I.; Topală, I.; Borcia, C.; Borcia, G. Adhesion Properties and Stability of Non-Polar Polymers Treated by Air Atmospheric-Pressure Plasma. *Polymers* **2023**, *15* (11), 2443.
- (44) Chen, G.; Zhang, Y.; Zhou, X.; Xu, J. Synthesis of Styrene—Maleic Anhydride Copolymer Esters and Their Surface Enriched Properties When Blending with Polyethylene. *Appl. Surf. Sci* **2006**, 253 (3), 1107–1110.
- (45) Li, B.; Zhang, J.; Ren, M.; Wu, P.; Liu, Y.; Chen, T.; Cheng, Z.; Wang, X.; Liu, X. Various Surface Functionalizations of Ultra-High-Molecular-Weight Polyethylene Based on Fluorine-Activation Behavior. *RSC Adv* **2015**, *5* (96), 79081–79089.

- (46) Wiphanurat, C.; Hanthanon, P.; Ouipanich, S.; Harnkarnsujarit, N.; Magaraphan, R.; Nampitch, T. Blending HDPE with Biodegradable Polymers Using Modified Natural Rubber as a Compatibilizing Agent: Mechanical, Physical, Chemical, Thermal and Morphological Properties. *Polym. Bull* **2023**, *80* (10), 11421–11437.
- (47) Zhao, Y.; Zhang, S.; Zhang, L.; Che, M.; Huang, R.; Cui, M.; Qi, W.; Su, R. Mechanical Properties and Interfacial Adhesion Mechanism of Polyolefin Composites Reinforced with Ethylene Vinyl Alcohol-Coated Cellulose Microfibers. *Chem. Eng. J.* **2025**, *506*, 159910.
- (48) Ye, W.; Wang, H.; Shen, J.; Khan, S.; Zhong, Y.; Ning, J.; Hu, Y. Halogen-Based Functionalized Chemistry Engineering for High-Performance Supercapacitors. *Chin. Chem. Lett* **2023**, *34* (1), 107198.
- (49) Marcano, A.; Fatyeyeva, K.; Koun, M.; Dubuis, P.; Grimme, M.; Chappey, C.; Marais, S. Enhanced Water and Oxygen Barrier Performance of Flexible Polyurethane Membranes for Biomedical Application. J. Biomed. Mater. Res., Part A 2022, 110 (1), 105–121.
- (50) Marais, S.; Hirata, Y.; Cabot, C.; Morin-Grognet, S.; Garda, M.-R.; Atmani, H.; Poncin-Epaillard, F. Effect of a Low-Pressure Plasma Treatment on Water Vapor Diffusivity and Permeability of Poly-(Ethylene-Co-Vinyl Alcohol) and Polyethylene Films. *Surf. Coat. Technol* **2006**, 201 (3–4), 868–879.
- (51) Zhang, Z.; Zhao, X.; Wang, S.; Zhang, J.; Zhang, W. Inducing a Network Structure of Rubber Phase: An Effective Approach to Toughen Polymer without Sacrificing Stiffness. *RSC Adv* **2014**, 4 (105), 60617–60625.
- (52) Mao, Z.; Zhang, J. Synergistic Toughening Effect of Chlorinated Polyethylene and Acrylic Resin on SAN/ASA Blends at Low Temperature. *J. Appl. Polym. Sci* **2016**, *133* (37), 43958.
- (53) Wu, S. Polar and Nonpolar Interactions in Adhesion. J. Adhes 1973, 5 (1), 39-55.
- (54) Cavallo, G.; Metrangolo, P.; Milani, R.; Pilati, T.; Priimagi, A.; Resnati, G.; Terraneo, G. The Halogen Bond. *Chem. Rev* **2016**, *116* (4), 2478–2601.
- (55) Van Krevelen, D. W.; Te Nijenhuis, K. Polymer Properties. In *Properties of Polymers*; Elsevier, 2009, pp. 3–5. DOI: .
- (56) Starostina, I. A.; Stoyanov, O. V.; Bogdanova, S. A.; Deberdeev, R. J.; Kurnosov, V. V.; Zaikov, G. E. Studies on the Surface Properties and the Adhesion to Metal of Polyethylene Coatings Modified with Primary Aromatic Amines. *J. Appl. Polym. Sci* **2001**, *80* (3), 388–397.
- (57) Thurston, R. M.; Clay, J. D.; Schulte, M. D. Effect of Atmospheric Plasma Treatment On Polymer Surface Energy and Adhesion. *J. Plast. Film Sheeting* **2007**, 23 (1), 63–78.
- (58) Ghanbari, A.; Attar, M. M. Surface Free Energy Characterization and Adhesion Performance of Mild Steel Treated Based on Zirconium Conversion Coating: A Comparative Study. *Surf. Coat. Technol* **2014**, 246, 26–33.
- (59) Yamauchi, K.; Shiotani, Y.; Saito, H. Deviation from Linear Relationship between Adhesion Strength and Surface Free Energy on a Low Energy Surface. *Procedia Struct. Integr* **2023**, *45*, 125–131.
- (60) Smith, T. Surface Energetics and Adhesion. *J. Adhes* **1980**, *11* (3), 243–256.

